Check for updates

OPEN

Polymerized human hemoglobin facilitated modulation of tumor oxygenation is dependent on tumor oxygenation status and oxygen affinity of the hemoglobin-based oxygen carrier

Donald A. Belcher[1,3], Alfredo Lucas[2,3], Pedro Cabrales[2] & Andre F. Palmer[1✉]

Administration of hemoglobin-based oxygen carriers (HBOCs) into the systemic circulation is a potential strategy to relieve solid tumor hypoxia in order to increase the effectiveness of chemotherapeutics. Previous computational analysis indicated that the oxygen (O_2) status of the tumor and HBOC O_2 affinity may play a role in increased O_2 delivery to the tumor. However, no study has experimentally investigated how low- and high-affinity HBOCs would perform in normoxic and hypoxic tumors. In this study, we examined how the HBOC, polymerized human hemoglobin (PolyhHb), in the relaxed (R) or tense (T) quaternary state modulates O_2 delivery to hypoxic (FME) and normoxic (LOX) human melanoma xenografts in a murine window chamber model. We examined microcirculatory fluid flow via video shearing optical microscopy, and O_2 distributions via phosphorescence quenching microscopy. Additionally, we examined how weekly infusion of a 20% top-load dose of PolyhHb influences growth rate, vascularization, and regional blood flow in the FME and LOX tumor xenografts. Infusion of low-affinity T-state PolyhHb led to increased tissue oxygenation, decreased blood flow, decreased tumor growth, and decreased vascularization in hypoxic tumors. However, infusion of both T-state and R-state PolyhHbs led to worse outcomes in normoxic tumors. Of particular concern was the high-affinity R-state PolyhHb, which led to no improvement in hypoxic tumors and significantly worsened outcomes in normoxic tumors. Taken together, the results of this study indicate that the tumor O_2 status is a primary determinant of the potency and outcomes of infused PolyhHb.

Unregulated angiogenesis and rapid cell proliferation in the tumor microenvironment result in decreased blood flow and oxygen (O_2) delivery[1]. Under these conditions, cancer cells adapt to the hypoxic environment via activation of hypoxia-inducible factors, HIF-1 and HIF-2[2]. These adaptations to chronic hypoxia are associated with metabolic reprogramming, angiogenesis, epithelial-mesenchymal transition, metastasis, and resistance to radiation and chemotherapy[3,4]. Furthermore, many forms of cancer therapy require reactive oxygen species (ROS) to promote tumor suppression[5]. Thus, increasing O_2 delivery to solid tumors is a promising target for cancer therapy.

[1]William G. Lowrie Department of Chemical and Biomolecular Engineering, The Ohio State University, Columbus, OH 43210, USA. [2]Department of Bioengineering, University of California San Diego, La Jolla, CA 92093, USA. [3]These authors contributed equally: Donald A. Belcher and Alfredo Lucas. ✉email: palmer.351@osu.edu

Due to their ability to modulate O_2 delivery from the circulatory system, hemoglobin-based oxygen carriers (HBOCs) are promising O_2 therapeutics that may increase the effectiveness of chemotherapy[6–12]. However, HBOCs are still not clinically approved despite decades of research[13,14]. The elevated renal toxicity and hypertension associated with previous generations of commercial HBOCs have mainly been attributed to this delay in development. Current improvements in reactor design and product purification are now able to exclude the low molecular weight (MW) HBOC fractions (< 250 kDa) that contributed to the toxicity of early generation HBOCs[15–18].

The chemical modifications that are necessary to make HBOCs safe for infusion typically alter the HBOC O_2 affinity[16,17,19–21]. For example, conjugating polyethylene glycol to the surface of hemoglobin (Hb) results in an increased O_2 affinity (P_{50}: 5–6 mm Hg) compared to unmodified Hb[22,23]. Alternatively, commercial polymerized Hbs (PolyHbs) prepared via glutaraldehyde or O-raffinose crosslinking in the tense (T) quaternary state all have significantly lower O_2 affinity (P_{50}: 30–40 mm Hg) compared to unmodified Hb[24–26]. Recently, we demonstrated that the O_2 affinity of PolyHbs could be controlled by polymerizing the Hb under fully oxygenated or deoxygenated conditions[16,17,21]. By fully oxygenating the Hb during polymerization, the PolyHb is effectively locked into the high O_2 affinity, relaxed quaternary state (R-state). Alternatively, polymerizing the Hb while deoxygenated locks the PolyHb into the low O_2 affinity, T-state.

Previously, we computationally determined that alterations in the O_2 affinity of the HBOC impact how much O_2 an HBOC will supply to the surrounding tumor tissue[20,27]. From the results of these studies, we anticipate that R-state PolyHb and T-state PolyHb should increase O_2 delivery to hypoxic tissue. Whereas in normoxic tissue, T-state PolyHb should increase oxygenation. To date, no study has examined how infusing an HBOC may impact the growth and vascularization of hypoxic and normoxic tumors. Previous studies only examined hypoxic tumors or a single class of HBOC[28–33]. Understanding how both normoxic and hypoxic tumors respond to different modes of enhanced O_2 delivery is vital to defining how these materials would be applied clinically.

In this work, we prepared high MW polymerized human Hbs (PolyhHbs) in either the T- or R-state. We then observed how each of these materials modulate O_2 transport within hypoxic (FME) and normoxic (LOX) human melanoma xenografts. By using the LOX melanoma cell line, we are able to generate normoxic tumors to compare with the hypoxic tumors[34,35]. By using phosphorescence quenching microscopy (PQM) on the microcirculatory environment observed within window chamber models, we explored how PolyhHbs modulate blood flow and O_2 transport in vivo. Additionally, we examined how weekly infusions of PolyhHb impact tumor growth and vascularization. With these results, we are better able to define how the oxygenation status of the tumor and the O_2 affinity of an HBOC will impact modulation of O_2 delivery.

Results

Biophysical properties of PolyhHbs.
The resulting properties of the PolyhHbs used in this study are shown in Fig. 1. The metHb levels of the resulting solutions were $5.8 \pm 0.8\%$ for 35:1 T-state PolyhHb and $4.2 \pm 0.9\%$ for 30:1 R-state PolyhHb. The concentration of both solutions was maintained at 100 ± 1.5 mg/mL. Polymerization under fully oxygenated conditions resulted in a significant increase in O_2 affinity for 30:1 R-state PolyhHb ($P_{50} = 1.31 \pm 0.07$ mmHg) compared to hHb ($P_{50} = 12.4 \pm 1.3$ mm Hg). In contrast, polymerization under completely deoxygenated conditions significantly decreased O_2 affinity ($P_{50} = 34 \pm 1.1$ mmHg). After polymerization, the rate of O_2 release is significantly slower when compared to unmodified hHb. The 30:1 R-state PolyhHb ($D = 38 \pm 5.3$ nm) was smaller than 35:1 T-state PolyhHb ($D = 63.7 \pm 7.3$ nm). Despite being larger on average, 35:1 T-state PolyhHb contained significantly more low MW species (0th, 1st order) compared to 30:1 T-state PolyhHb.

Hematological and blood gas parameters.
Changes in hematological and blood gas parameters are displayed in Table 1. There were no differences in systemic blood parameters at baseline compared to healthy mice (no implanted tumor). Infusion of 35:1 T-state and 30:1 R-state PolyhHb significantly reduced the hematocrit. There was no significant difference between either the hematocrit or PolyhHb in the plasma after infusion of either 35:1 T-state or 30:1 R-state PolyhHb. Infusion of both 35:1 T-state PolyhHb and 30:1 R-state PolyhHb resulted in significant increases in MAP. In mice implanted with FME tumors, infusion of 30:1 R-state PolyhHb led to a significant decrease in HR compared to the Baseline. Similarly, in mice implanted with FME tumors, there was a significant increase in PaO_2 after infusion of 30:1 R-state PolyhHb compared to the baseline and 35:1 T-state PolyhHb treatment groups. In both tumors, infusion of 30:1 R-state PolyhHb led to a significant increase in $PaCO_2$ and a significant decrease in pH compared to both the baseline and 35:1 T-state PolyhHb treatment groups.

Tissue O_2 tension.
Changes in tissue O_2 tension in both hypoxic (FME) and normoxic (LOX) tumors are depicted in Fig. 2. The average tissue pO_2 of hypoxic (FME) tumors was significantly lower than the average tissue pO_2 in normoxic (LOX) tumors and host tissue. Infusion of 30:1 R-state PolyhHb significantly decreased tissue oxygenation in both normoxic (LOX) and hypoxic (FME) tumors compared to baseline and following infusion of 35:1 T-state PolyhHb. In contrast, infusion 35:1 T-state PolyhHb led to significant increases in average tissue pO_2 in both tumors.

Microhemodynamics.
Changes in the arteriolar and venular blood flow in both hypoxic (FME) and normoxic (LOX) tumors are depicted in Fig. 3A, B. Vessel diameters were separated into two groups for this analysis: one group with diameters less than 30 μm and another group with diameters greater than 30 μm. In hypoxic tumors, infusion of 30:1 R-state PolyhHb led to a significant reduction in the volumetric flow rate in small diameter ($D_{ves} < 30$ μm) venules. Infusion of 35:1 T-state PolyhHb led to significant increases in the flow
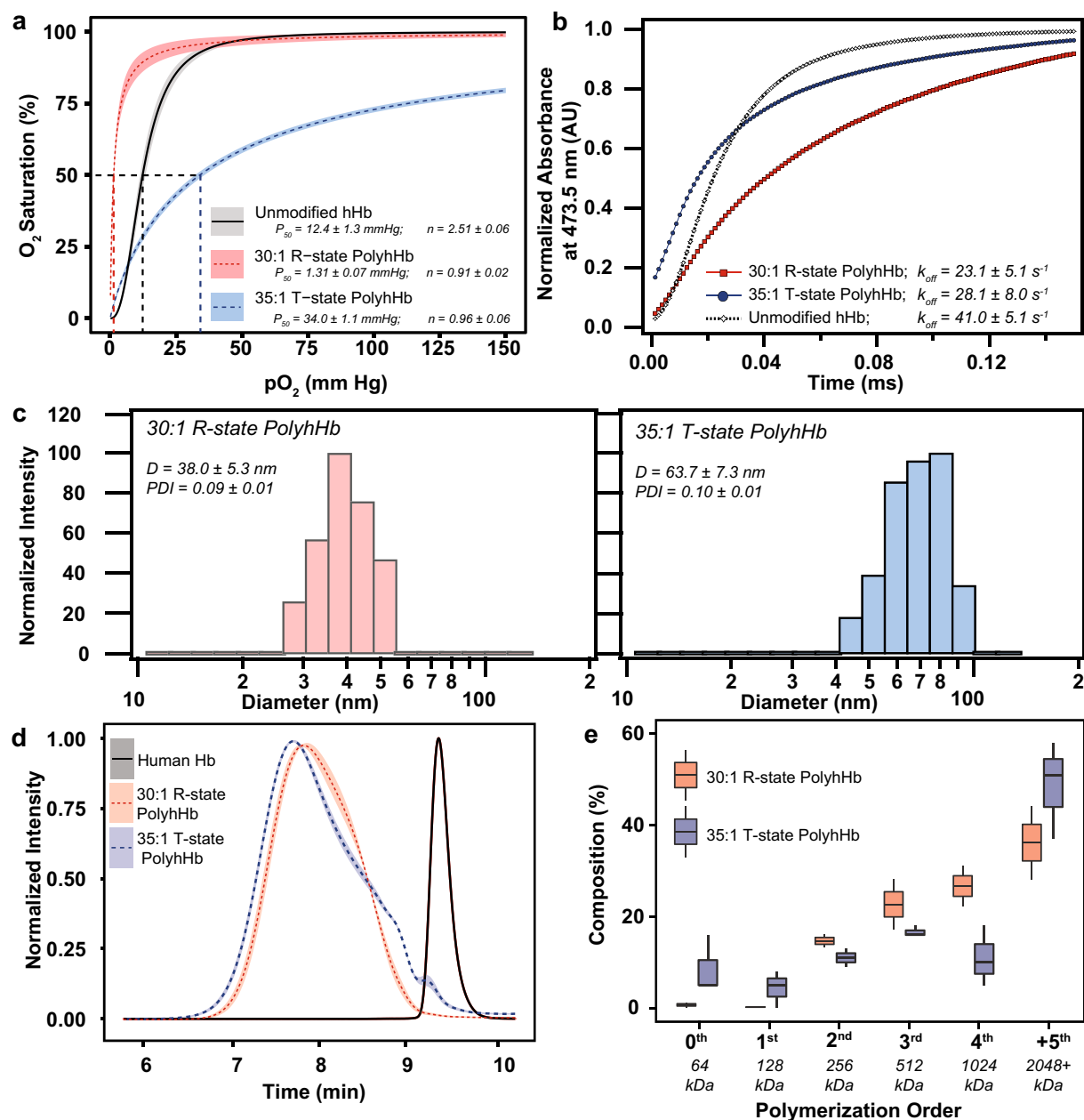
Figure 1. Biophysical properties of unmodified hHb, 35:1 T-state PolyhHb, and 30:1 R-State PolyhHb. (**A**) OECs for PolyhHb and hHb. (**B**) Comparison of the kinetic time course for deoxygenation in the presence of 1.5 mg/mL sodium dithionite for hHb, 30:1 R-state PolyhHb, and T-state PolyhHb. For OECs (**A**), The shaded region represents the 95% confidence interval for each quaternary state with three runs per sample. For deoxygenation (**B**), the experimental data shows an average of 10–15 kinetic traces. For deoxygenation, the reactions were monitored at 437.5 nm and 20 °C in 0.1 M pH 7.4 PBS. Symbols represent experimental data, and corresponding lines of the same color represent curve fits. (**C**) Representative intensity distributions of the hydrodynamic diameter of 30:1 R-state and 35:1 T-state PolyhHb. (**D**) Normalized SEC intensity distributions of R-state and T-state PolyhHb compared to unmodified hHb. The shaded region represents the 95% confidence interval for the average of the produced PolyhHb. (**E**) Polymer order distribution for 35:1 T-state and 30:1 R-state PolyhHb. Polymer distribution was calculated on a percent by heme basis via analysis of the 413 nm absorbance wavelength. The corresponding approximate sizes of the polymer orders are shown below each group.

rate in large diameter ($D_{ves} > 30$ μm) venules. In normoxic tumors, infusion of both PolyhHb species led to significant increases in tumor perfusion in all blood vessels. In general, blood flow velocity in normoxic tumors was significantly higher than blood flow in hypoxic tumors.

Parameter	Healthy	FME human melanoma xenograft			LOX human melanoma xenograft		
		Baseline	35:1 T-state PolyhHb	30:1 R-state PolyhHb	Baseline	35:1 T-state PolyhHb	30:1 R-state PolyhHb
Hb (g/dL)	14.6 ± 0.2	$14.6 \pm 0.2^{\ddagger}$	$10.8 \pm 0.4^{\dagger}$	$11.3 \pm 0.5^{\dagger}$	$14.6 \pm 0.2^{\ddagger}$	$10.9 \pm 0.2^{\dagger}$	$10.9 \pm 0.2^{\dagger}$
Plasma PolyhHb (g/dL)	–	–	1.4 ± 0.1	1.3 ± 0.1	–	1.3 ± 0.1	1.5 ± 0.1
MAP (mmHg)	105 ± 7	$104 \pm 6^{\ddagger}$	$122 \pm 4^{\dagger}$	$126 \pm 9^{\dagger}$	$105 \pm 8^{\ddagger}$	$128 \pm 5^{\dagger}$	$125 \pm 9^{\dagger}$
HR (beats/min)	517 ± 28	514 ± 26	492 ± 25	$469 \pm 28^{\dagger}$	518 ± 25	484 ± 27	496 ± 22
PaO$_2$ (mmHg)	106 ± 5	105 ± 5	97 ± 7	$113 \pm 8^{\dagger\ddagger}$	106 ± 7	$100 \pm .3$	107 ± 7
PaCO$_2$ (mmHg)	34.7 ± 1.9	35.0 ± 2.2	35.1 ± 2.0	$32.0 \pm 1.3^{\dagger\ddagger}$	34.5 ± 1.6	34.9 ± 1.5	$32.3 \pm 2.5^{\dagger\ddagger}$
pH	7.29 ± 0.09	$7.32 \pm 0.10^{\ddagger}$	$7.38 \pm 0.09^{\dagger}$	$7.25 \pm 0.12^{\dagger\ddagger}$	$7.29 \pm 0.07^{\ddagger}$	$7.35 \pm 0.10^{\dagger}$	$7.26 \pm 0.10^{\dagger\ddagger}$

Table 1. Hematological and blood gas parameters for healthy animals and animals implanted with FME or LOX tumor infused with a 20% top-load dose of either 35:1 T-state PolyhHb or 30:1 R-state PolyhHb. $^{\dagger}P < 0.05$ compared to baseline. $^{\ddagger}P < 0.05$ compared to 35:1 T-state PolyhHb (n = 6 mice).
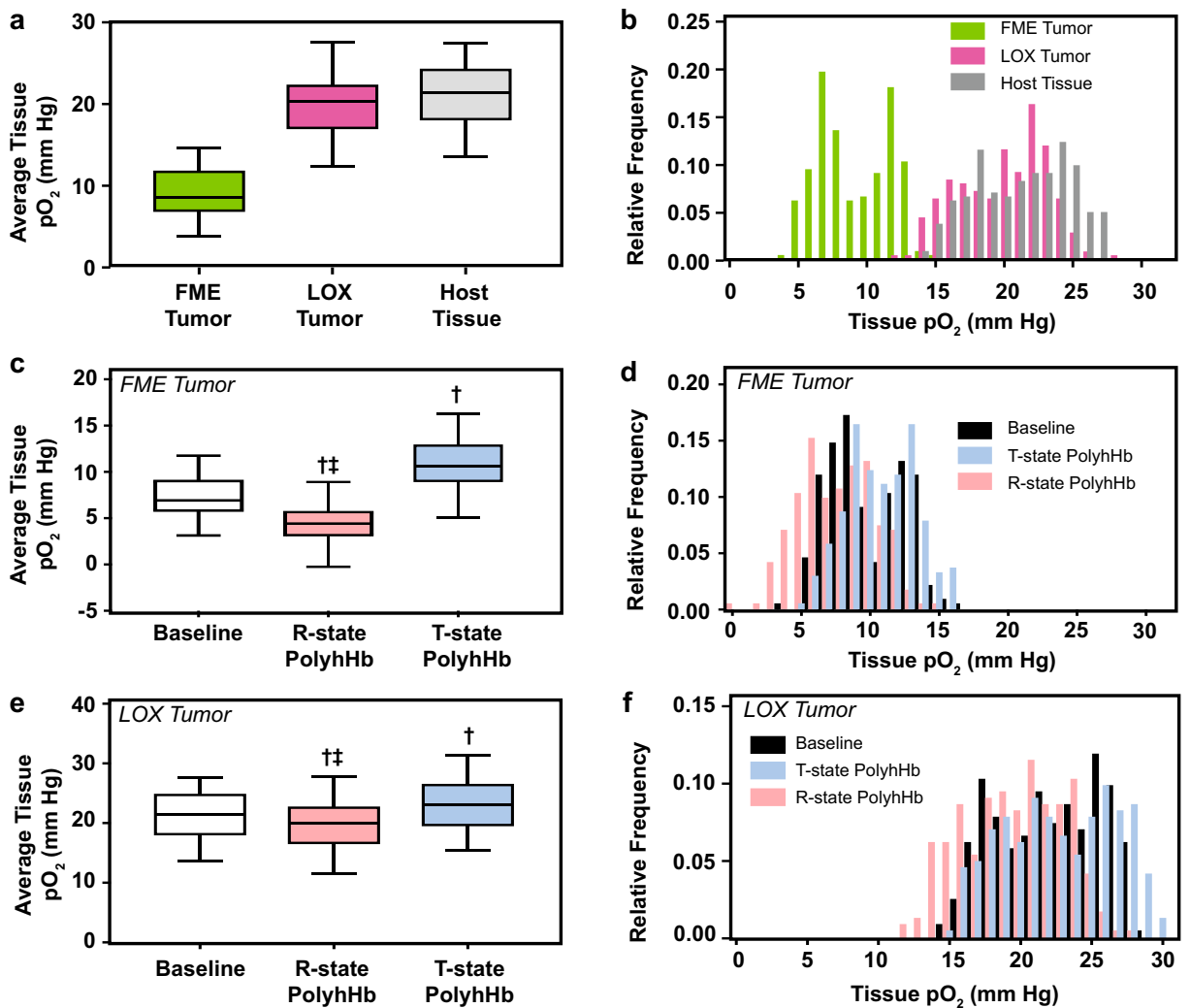

Figure 2. Average tissue pO$_2$ and distribution of measured tissue pO$_2$ in host tissue, and in hypoxic, and normoxic tumor xenografts as measured via phosphorescence quenching microscopy in the chamber window model. This figure shows the (**A**, **C**) average pO$_2$s and (**B**, **D**) frequency of tissue pO$_2$ for (**A**, **B**) hypoxic FME human melanoma and (**C**, **D**) normoxic LOX human melanoma tumor xenografts. Data is shown for the baseline and after infusion of 30:1 R-state PolyhHb and 35:1 T-state PolyhHb. $^{\dagger}P < 0.05$ compared to baseline. $^{\ddagger}P < 0.05$ compared to 35:1 T-state PolyhHb. (n = 5 mice).
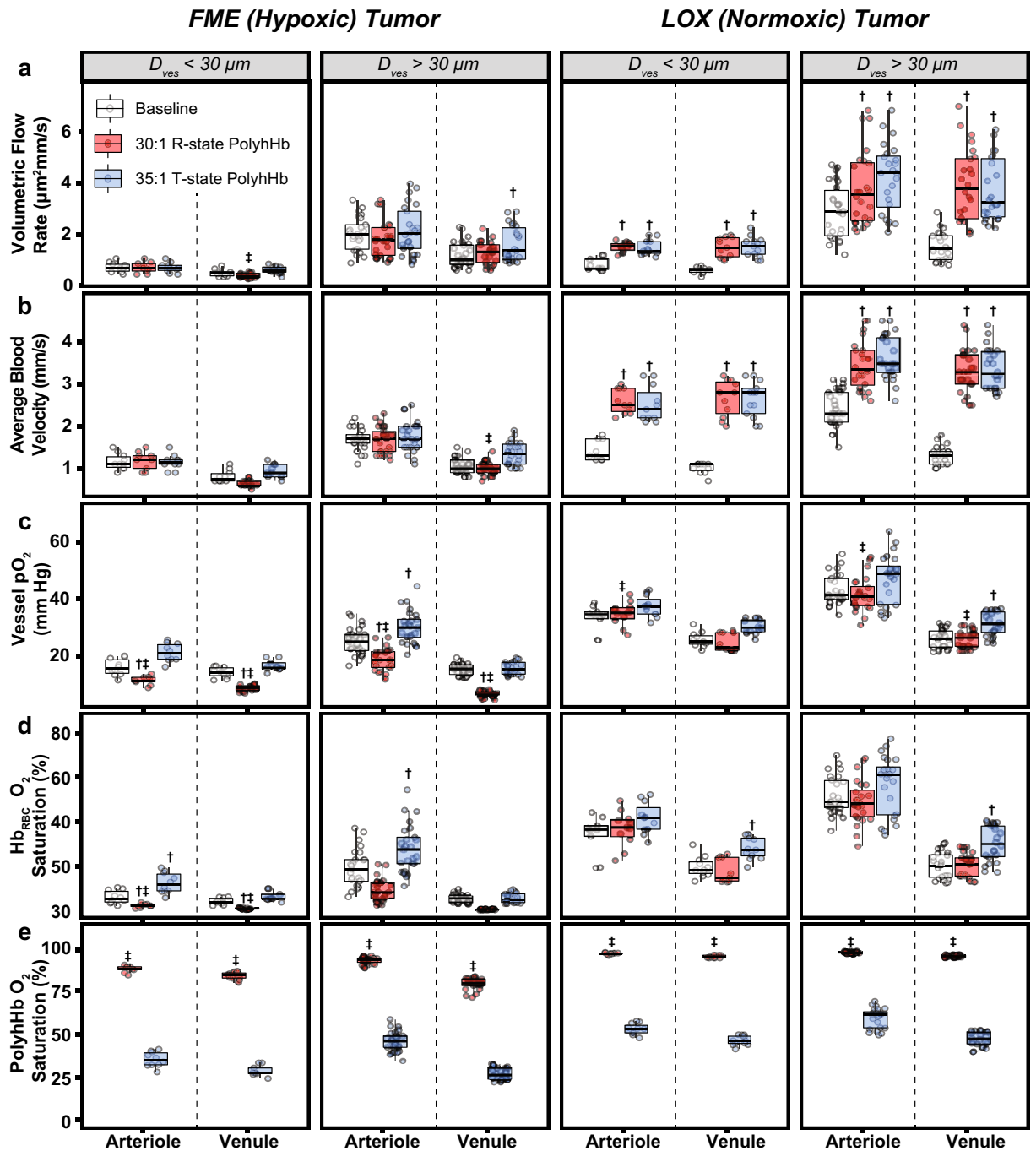
Figure 3. Results from the analysis of how PolyhHb modulates fluid and O_2 transport as measured in a murine chamber window model containing either hypoxic or normoxic tumors. This figure shows (**A**) volumetric flow rate through a blood vessel, (**B**) average blood velocity through the blood vessel, (**C**) average pO_2 in the blood vessel, (**D**) O_2 saturation of Hb in RBCs, and (**E**) O_2 saturation of PolyhHb in the plasma in hypoxic (FME) and normoxic (LOX) tumors. Vessels have been grouped by whether they flow into (arteriole) or out of (venule) the tumor along with whether the vessel is small (<30 μm) or large (>30 μm). †$P<0.05$ compared to baseline. ‡$P<0.05$ compared to 35:1 T-state PolyhHb. (n = 5 mice).

Intravascular pO_2 and O_2 saturations. Changes in intravascular pO_2, O_2 saturation of Hb in RBCs, and O_2 saturation of PolyhHbs are shown in Fig. 3C–E. The O_2 saturation of Hb in RBCs was always significantly greater in the normoxic tumor compared to the hypoxic tumor. Infusion of 30:1 R-state PolyhHb led to significant reduction in blood O_2 saturation in hypoxic tumors compared to both the control and infusion of 35:1 T-state PolyhHb. This is coupled with a corresponding significant ($P<0.05$) decrease in O_2 saturation of Hb in RBCs compared to the control and infusion of 35:1 T-state PolyhHb. Infusion of 35:1 T-state PolyhHb leads to a significant increase in intravascular pO_2 in large diameter ($D_{ves}>30$ μm) arterioles in the hypoxic tumor and
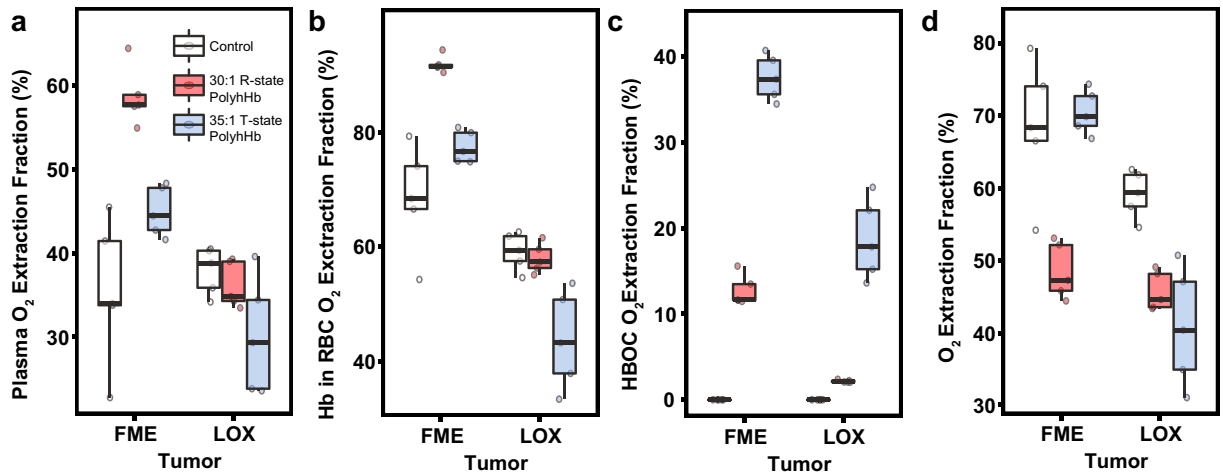
Figure 4. Oxygen extraction fraction from various species as measured in a murine chamber window model containing either hypoxic or normoxic tumors. This figure displays the oxygen extraction fraction (OEF) as a percentage of total inlet oxygen (O_2) for (**A**) O_2 dissolved in the plasma, (**B**) O_2 bound to Hb in RBCs, (**C**) O_2 bound to PolyhHbs, and (**D**) total O_2 from all O_2 carrying species in hypoxic (FME) and normoxic (LOX) tumors. [†]$P < 0.05$ compared to baseline. [‡]$P < 0.05$ compared to treatment with 35:1 T-state PolyhHb. (n = 5 mice).

large diameter ($D_{ves} > 30$ μm) venules in the normoxic tumor. Additionally, infusion of 35:1 T-state PolyhHb significantly ($P < 0.05$) increased O_2 saturation of Hb in RBCs in the arterioles of hypoxic tumors and the venules of normoxic tumors. As anticipated, the O_2 saturation of 30:1 R-state PolyhHb was always significantly greater than the O_2 saturation of 35:1 T-state PolyhHb.

Oxygen extraction fraction (OEF). The changes in the calculated plasma OEF, Hb in RBC OEF, PolyhHb OEF, and overall OEF in hypoxic (FME) and normoxic (LOX) tumors are displayed in Fig. 4. Infusion of 30:1 R-state PolyhHb significantly increased the amount of O_2 extracted from plasma and RBCs in hypoxic (FME) tumors. Infusion of 35:1 T-state PolyhHb led to a significant reduction in the OEF from plasma and Hb in RBCs. The OEF from 35:1 T-state PolyhHb was significantly greater than the O_2 extraction from 30:1 R-state PolyhHb. Infusion of 30:1 R-state PolyhHb decreased overall OEF in both hypoxic (FME) and normoxic (LOX) tumors. Infusion of 35:1 T-state PolyhHb led to significant reduction in overall OEF in LOX tumors; however, it did not lead to any significant changes in the OEF in FME tumors.

Tumor growth. In addition to examining how PolyhHb altered microvascular O_2 transport in tumors, we also examined how a low volume weekly dose of 30:1 R-state PolyhHb and 35:1 T-state PolyhHb would impact tumors implanted into tissue. The effects of weekly 20% top-load doses of 30:1 R-state PolyhHb and 35:1 T-state PolyhHb on the volumes of FME and LOX tumor xenografts are shown in Fig. 5. The approximate rate of radial expansion was approximately 5.5 μm/h for FME (hypoxic) tumors and approximately 4.1 μm/h for LOX (normoxic) tumors. After top-load infusion of both T-state and R-state PolyhHb, there is a significant reduction in the growth of the hypoxic FME tumor. Infusion of 35:1 T-state PolyhHb resulted in a significant reduction in FME tumor growth (20%) compared to 30:1 R-state PolyhHb (9.6%).

Tumor vasculature. We were also interested in experimentally observing how periodic infusions of PolyhHb solutions would alter properties associated with microvascular mass transport. Regional blood flow (RBF) was analyzed with fluorescent microsphere perfusion, and microvascular density (MVD) was estimated via tissue histology. The results of these studies are shown in Fig. 5B, C. In hypoxic FME tumor xenografts, infusion of 35:1 T-state PolyhHb led to a significant decrease in both RBF and MVD. In normoxic LOX tumor xenografts, infusion of T-state PolyhHb led to a significant increase in RBF to the tumor compared to baseline.

Discussion

The principal finding of this study is that the O_2 status of tumors has a strong effect on the effects of PolyhHb coadministration. These results may help explain some of the previous negative results that occurred in rhabdomyosarcomas[28].

In this study, we investigated how infusion of PolyhHb influences microcirculatory fluid and O_2 transport within a murine chamber window model. In general, infusion of 35:1 T-state PolyhHb led to increased tumor perfusion and O_2 delivery. In contrast, infusion of 30:1 R-state PolyhHb decreased overall fluid and O_2 transport. This can be attributed to two factors: (1) 30:1 R-state PolyhHb had extremely high O_2 affinity, and (2) 30:1 R-state PolyhHb was slightly hypertensive. After infusion of 30:1 R-state PolyhHb there was a significant increase in MAP and PaO_2 coupled with a decrease in $PaCO_2$, HR, and pH. In comparison, infusion of 35:1 T-state PolyhHb

6
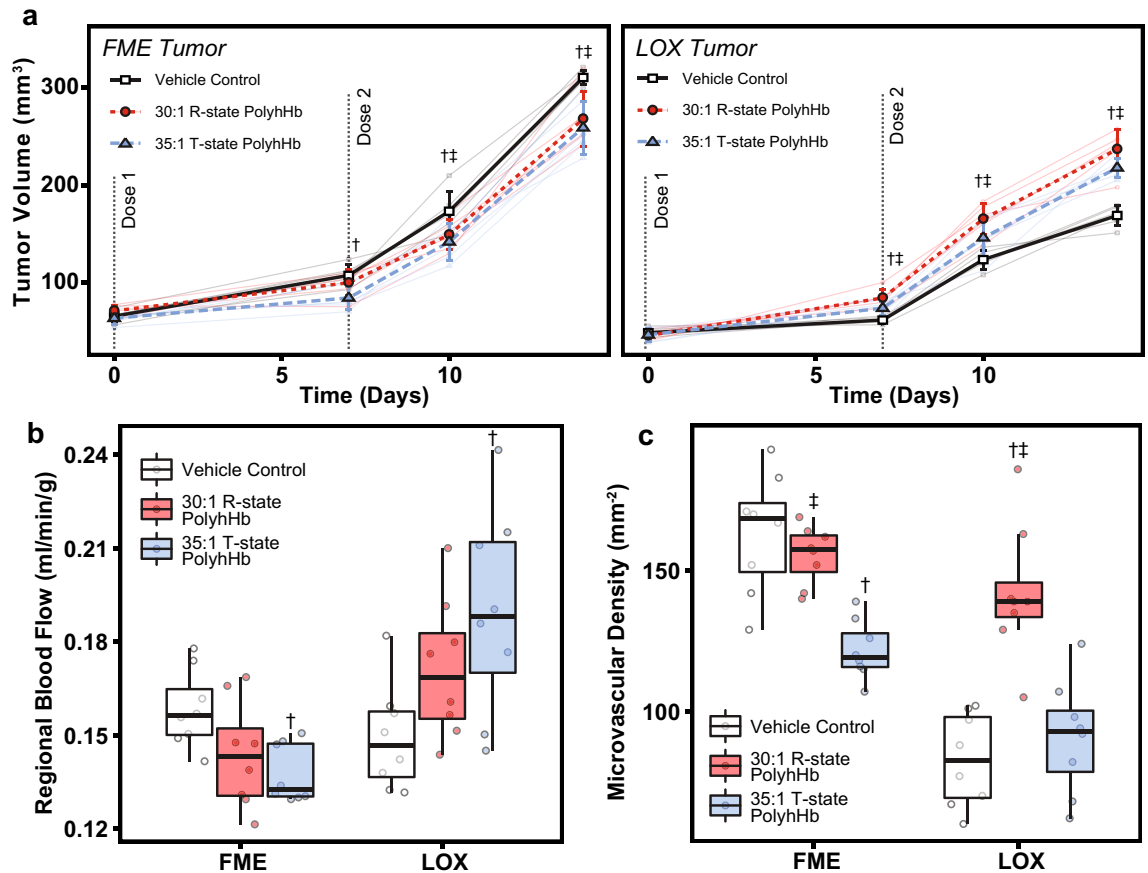
Figure 5. Tumor properties after weekly PolyhHb infusions. (**A**) Volume expansion of hypoxic and normoxic tumor xenografts over two weeks after weekly infusion of 35:1 T-state, 30:1 R-state PolyhHb, or the vehicle control to (LEFT) hypoxic FME and (RIGHT) normoxic LOX human melanoma tumor xenografts. Grey lines connect tumor growth measured in the same animal. (**B**) Microvascular density measured at the end of tumor growth after weekly administration of PolyhHb. (**C**) Regional blood flow after weekly administration of PolyhHb. (**D**) Microvascular density (represented as the density of competent vessels in the viewing area) after weekly infusion of PolyhHb or the vehicle control. †$P < 0.05$ compared to baseline. ‡$P < 0.05$ compared to treatment with 35:1 T-state PolyhHb.

primarily increased MAP. These increases in MAP is consistent with previous HBOCs containing low MW species[36,37].

In normoxic tumors, the hemodulution effect of PolyhHb infusion led to significant increases in tumor perfusion. Despite this increase in blood perfusion after the infusion of R-state PolyhHb, the average tissue pO_2 decreased. This decrease is likely a result of the relatively low amount of O_2 extracted from R-state PolyhHb ($2.2 \pm 0.1\%$), which failed to make up for the lack of O_2 carrying capacity from the diluted blood. In comparison, $18.7 \pm 4.7\%$ of the total available O_2 from T-state PolyhHb was extracted, which offset the O_2 extraction from both Hb in RBCs and dissolved O_2 in plasma.

In hypoxic tumors, the percentage of O_2 extracted from 30:1 R-state PolyhHb only slightly increased ($12.8 \pm 1.8\%$) compared to the percentage of O_2 extracted from 35:1 T-state PolyhHb ($37.5 \pm 2.6\%$). This slight increase in O_2 extraction from R-state PolyhHb does not fully offset the O_2 demand from O_2 dissolved in plasma and Hb in RBCs. When the decrease in O_2 supply from R-state PolyhHb is coupled with reduced blood flow resulting from vasoconstriction, overall O_2 delivery is significantly reduced. This requirement is instead offset by significant increases in the O_2 extracted by the dissolved O_2 in the plasma and Hb in RBCs.

In this study, we found that the infusion of PolyhHb led to relatively minor changes in the growth rate of the hypoxic (FME) tumors. However, it appears that this low dosage was unable to replicate the significant reduction in tumor growth (40%) that was previously observed in a triple-negative breast cancer model[20]. This is likely because the dose volume and dose frequency were too low to result in an appreciable effect on tumor growth. For this study, the PolyhHb was delivered weekly; however, previous studies of the pharmacokinetics of similar PolyhHbs indicate that these PolyhHbs have a half-life of only 24 h[15]. Taking this into account, the tumors were only exposed to the O_2 modulating effect of PolyhHb for only 25% of the week. Increasing the dosing frequency to once every 2 to 3 days may increase the relative effect.

Unfortunately, infusion of both the T-state and R-state PolyhHb solutions led to a significant increase in tumor growth for normoxic LOX tumors. Infusion of 30:1 R-state PolyhHb led to a 40% increase in tumor volume after the 14-day treatment regime. This is likely because both 35:1 T-state PolyhHb and 30:1 R-State PolyhHb

have higher O_2 affinity compared to mouse Hb in RBCs ($P_{50} = 42$ mm Hg). Because of this relative increase in O_2 affinity, we anticipate that less O_2 may be delivered under normoxic conditions, which could decrease host cell survival in the tumor periphery. We anticipate that when applied to a model that more accurately represents human physiology, T-state PolyhHb might decrease the tumor growth rate due to its lower O_2 affinity compared to human Hb in RBCs ($P_{50} = 26$ mm Hg). However, we may also observe further increases in tumor growth due to the increased supply of O_2 to normoxic tumors.

Despite observing a growth delay after infusion of 30:1 R-state PolyhHb, infusion of R-state PolyhHb did not lead to significant decreases in RBF or MVD. This is likely because the low dose frequency and high O_2 affinity of R-state PolyhHb were insufficient to trigger an anti-angiogenic response in FME tumors. Baseline values for RBF in hypoxic FME tumors [0.16 ± 0.02 mL/(min g)] and normoxic LOX tumors [0.15 ± 0.02 mL/(min g)] are at the upper range of the values measured for other tumors experimentally[38–40]. In the hypoxic (FME) tumors, we observed decreases in MVD after delivery of 35:1 T-state PolyhHb. This decrease in vessel formation indicates an increase in O_2 delivery. In contrast, we observed a significant increase in MVD after weekly infusions of 30:1 R-state PolyhHb in normoxic (LOX) tumors. This is consistent with a decrease in O_2 delivery, which may lead to more aggressive tumor growth and increased angiogenesis. In fact, the MVD of the normoxic LOX tumor after infusion of 30:1 R-state PolyhHb is remarkably similar to the measured MVD within the baseline hypoxic (FME) tumor. This further supports the notion that within the normoxic tumor, R-state PolyhHb is not adequately delivering O_2, which is in agreement with microvascular simulations performed previously[20]. Despite this, reduction in tumor growth has been previously observed after infusion of high O_2 affinity HBOCs[41–43]. Therefore, this decrease in tumor growth may be due to other factors in the environment including production of reactive O_2 species (ROS)[44] and nitric oxide (NO) scavenging[45]. This faster rate of metHb formation will lead to the increased production of ROS which can induce oxidative injury to the tumor mass. This is especially important to consider given that HBOCs can scavenge NO[46] and can oxidize and produce ROS[47] species in vivo. Future studies should investigate these mechanisms in more detail by directly observing changes in hypoxia inducible factors and downstream proteins when working with high O_2 affinity HBOCs.

Conclusions

The results from this study indicate that low-dose, infrequent infusions of R-state PolyhHb is not suitable for oxygenating both hypoxic and normoxic melanomas. In general, treatment of normoxic tumors with either high- or low O_2 affinity PolyhHbs aggravated tumor growth and angiogenesis. In contrast, T-state PolyhHbs significantly increased O_2 supply to hypoxic tumors. These results encourage the use of low O_2 affinity PolyhHbs with reduced cooperativity to hypoxic tumors. Additionally, this further emphasizes the need to fully characterize how different tumor types respond to modulating O_2 delivery with HBOCs.

Methods

Polymerized hemoglobin synthesis and analysis.   Human Hb (hHb) used in these studies was first purified from human red blood cells (RBCs) as described previously[48]. PolyhHb was produced using methods described previously[17]. In brief, the resulting hHb solution was polymerized with glutaraldehyde while fully oxygenated or deoxygenated to form either R-state or T-state PolyhHb, respectively. The resulting PolyhHbs were first clarified on a 0.2 μm hollow fiber filter. After clarification, the PolyhHb solutions were diafiltered on a 100 kDa hollow fiber filter into a modified Ringer's lactate buffer to remove the low MW PolyhHb/hHb species. The cyanomethemoglobin method was used to measure the Hb concentration and the metHb level of hHb/PolyhHb solutions[49,50]. The size distribution of PolyhHb, by particle volume, was measured using dynamic light scattering (DLS) (Brookhaven Instrument Inc. BS-200M, Holtsville, NY). The O_2-hHb/PolyhHb equilibrium binding curves were measured using a Hemox Analyzer (TCS Scientific Corp., New Hope, PA). The hHb/PolyhHb kinetics of O_2 offloading (k_{off,O_2}) were measured with an Applied Photophysics SF-17 microvolume stopped-flow spectrophotometer (Applied Photophysics Ltd., Surrey, United Kingdom) using protocols previously described by Rameez and Palmer[51–53]. The MW distribution was estimated using an Acclaim SEC-1000 column (Thermo Scientific, Waltham, MA) on a Thermo Scientific Dionex Ultimate UHPLC system using previously described methods[17,54].

Dorsal chamber window model.   Adult female 8- to 10-week old female BALB/c-nu/nu mice were used for the xenografted tumors according to protocols approved by the University of California San Diego Animal Care and Use Committee. Mice were instrumented with dorsal chamber windows as described previously[55,56]. This experimental model is an excellent system to observe O_2 delivery as it is highly sensitive to changes in O_2 supply[57]. Additionally, this model is especially useful when examining changes in microvascular pO_2 distributions in the unanesthetized state. Human melanomas (FME and LOX) were initiated by implanting a 200–500 μm xenograft into the fascial side of the intact skin layer of the chamber window model. FME and LOX cells were generously donated by Micro-Target Dynamic Therapy (San Diego, CA). The FME and LOX human melanoma cell lines were originally developed by the Rofstad Group at the Institute for Cancer Research (Oslo University Hospital, Norway)[34,35]. After implantation of the xenografts, tumors were allowed to grow for 7 days before analysis. Mice were divided into two groups based on the implanted human tumor cell lines (FME or LOX). Each of these groups was further subdivided into three cohorts: (1) an unsupplemented baseline, (2) infusion of 30:1 R-state PolyhHb, and (3) infusion of 35:1 T-state PolyhHb. At this point, mice underwent a 20% top load (20% of the mouse blood volume calculated by weight) infusion of a 30:1 R-state PolyhHb or a 35:1 T-state PolyhHb at a concentration of 100 mg/mL. PolyhHb was infused via tail vein injection. After infusion, the animal was placed into a restraining tube. Once in the tube, the protruding chamber window was fixed to a microscopic stage of a BX51WI intravital microscope (Olympus, New Hyde Park, NY). Tissue images were

then projected to a 4,815 charge-coupled device camera (Cohu Industries, Poway, CA). A LUMPFL-WIR×40 numerical 0.8 aperture water immersion objective (Olympus, New Hyde Park, NY) was used to carry out the measurements. Mean arterial pressure (MAP) and heart rate (HR) were recorded using a pressure transducer connected to the femoral artery catheter using an MP-150 system (BIOPAC Systems, Goleta, CA). Arterial blood was collected in heparinized capillary tubes and immediately analyzed for PaO_2, $PaCO_2$, and pH using a 248 Blood Chemistry Analyzer (Bayer, Norwood, MA). Total Hb was measured spectrophotometrically using a B-hemoglobin Hemocue (Stockholm, Sweden). Plasma Hb was measured from plasma collected after the capillary tube was centrifuged.

Phosphorescence quenching microscopy (PQM). Phosphorescence quenching microscopy (PQM) was used to analyze the O_2 distribution in the tissue and vascular space, as described previously[58]. This high-resolution method allows us to resolve the pO_2 of arterioles and venules within the growing tumor. To determine the pO_2 in this method, we measure the decay rate of the excited palladium-mesotetra-(4-carboxyphenyl) porphyrin (Frontier Scientific Porphyrin Products, Logan, UT) bound to albumin. We then used the measured fluorescence lifetime (τ_p), fluorescence lifetime in the absence of O_2 ($\tau_{p,0}$), and fluorescence quenching rate constant (k_q) to calculate the pO_2 using the Stern–Volmer equation, as shown in Eq. (1)[59].

$$pO_2 = \frac{\left(\frac{\tau_{p,0}}{\tau_p - 1}\right)}{\tau_{p,0} k_q} \tag{1}$$

The probe was injected intravenously 10 min before pO_2 distributions were measured to allow time for the phosphorescent probe to circulate and diffuse into the chamber window model. The exposed tissue within the chamber window was then excited with 420 nm wavelength light. To acquire τ_p, the 680 nm emitted phosphorescence signal was collected. Because this method is relatively independent of the probe concentration, we were also able to measure extravascular tissue pO_2.

Microvascular hemodynamics. To observe changes in the arteriole and venule diameter, we used a video image shearing method to determine blood vessel diameter[60]. Center-line velocities of arterioles and venules were measured with a 102B Vista Electronics photo-diode velocity tracker (San Diego, CA) using a cross-correlation method. Volumetric flow rate (Q) through the arterioles and venules was then calculated using the radius of the vessel (r_{ves}) and average fluid velocity (v_f), as described in Eq. (2). For these calculations, we assume that fluid velocity profile was parabolic in arterioles and venules.

$$Q = \pi \bar{v}_f r_{ves}^2 \tag{2}$$

We are also able to calculate the oxygen extraction fraction (OEF) from the various species (dissolved oxygen, RBCs, PolyhHb) in solution by calculating the average mass flux of O_2 into the tumor subtracted by the blood flow normalized average mass flux of O_2 out of the tumor. The resulting O_2 mass deficit is then divided by the average mass flux of O_2 into the tumor as shown in Eq. (3).

$$OEF = \frac{\frac{\sum [O_{2,in}]_i Q_{in}}{n} - \frac{\sum [O_{2,out}]_i Q_{out}}{n} \times \frac{\sum Q_{in}}{\sum Q_{out}}}{\sum [O_{2,in}]_i Q_{in}} \tag{3}$$

Tumor growth model. Similar to the chamber window model study, adult 8- to 10-week old female BALB/c-nu/nu mice were used for the xenografted tumors according to protocols approved by the University of California San Diego Animal Care and Use Committee. Approximately 4×10^5 cells of the human melanoma cell lines FME and LOX were injected into the mouse flank. Mice were divided upon the tumor cell lines (FME or LOX). Each of these groups was further subdivided into three cohorts: (1) an unsupplemented baseline, (2) infusion of 30:1 R-state PolyhHb. and (3) infusion 35:1 T-state PolyhHb. Mice were infused with the 100 mg/mL PolyhHb solutions via tail vein injection of 20% of the mouse's blood volume once each week during the study. During tumor growth, the length of the tumor (L_{tumor}) and width of the tumor (W_{tumor}) were both measured to estimate tumor volume as shown in Eq. (4).

$$V_{tumor} = \frac{\pi L_{tumor} W_{tumor}^2}{6} \tag{4}$$

Tumor blood flow. Fluorescently labeled microspheres were used to estimate tumor blood flow in tumors as described previously[61]. In short, 15 µm diameter fluorescent microspheres (Molecular Probes, Eugene, OR) were suspended in saline. 100 µL of this solution was rapidly injected into the animal via the tail vein. Arterial reference samples were simultaneously withdrawn at a constant rate of 100 µL/min for 1 min through an inserted femoral catheter. At the end of the protocol, the mice were euthanized with a lethal dose of sodium pentobarbital. Tumor tissue was then digested in 1 M KOH solution for 24 h. Fluorescent dye was extracted with Cellosolve (Fisher Scientific, Pittsburgh, PA). The fluorescent signal was then measured using an LS 50B luminescence spectrometer (PerkinElmer Corp., Norwalk, CT). Regional blood flow proportional to the fraction of cardiac output was calculated by measuring the number of fluorescent microspheres in the tumor tissue relative to the total in the arterial reference samples.

Tumor histopathology. Harvested tumors were fixed in PBS 4% paraformaldehyde, embedded in paraffin cases, cut into sections, and stained. Vascular density was assessed by counting the number of capillary profiles within a 0.8 mm^2 field of view. Positive capillaries were only counted if a lumen and a brown staining endothelial cell were identified.

Statistical analysis. All results are presented as the mean ± standard deviation. Statistically significant changes were analyzed with two-way ANOVA followed by post-hoc analysis using Tukey's multiple comparison test when appropriate. All statistics were calculated with R (v 3.6.2). Results were considered statistically significant if $P < 0.05$.

Ethics approval. All experimental protocols used to handle the mice were approved by the University of California San Diego Institutional Animal Care and Use Committee. The Hb used to prepare these materials was purified from expired RBCs donated from the Wexner Medical Center (Columbus, OH).

Data availability

The datasets generated during and/or analysed during the current study are available from the corresponding author on reasonable request.

References

1. Moulder, J. E. & Rockwell, S. Tumor hypoxia: its impact on cancer therapy. *Cancer Metastasis Rev.* **5**, 313–341 (1987).
2. Semenza, G. L. Hypoxia-inducible factors in physiology and medicine. *Cell* **148**, 399–408 (2012).
3. Semenza, G. L. Defining the role of hypoxia-inducible factor 1 in cancer biology and therapeutics. *Oncogene* **29**, 625–634 (2010).
4. Semenza, G. L. Targeting HIF-1 for cancer therapy. *Nat. Rev. Cancer* **3**, 721–732 (2003).
5. Schumacker, P. T. Reactive oxygen species in cancer: a dance with the devil. *Cancer Cell* **27**, 156–157 (2015).
6. Robinson, M. F. *et al.* Increased tumor oxygenation and radiation sensitivity in two rat tumors by a hemoglobin-based, oxygen-carrying preparation. *Artif. Cells Blood Substit. Biotechnol.* **23**, 431–438 (1995).
7. Teicher, B. A. *et al.* Effect of a bovine hemoglobin preparation (sbhs) on the response of two murine solid tumors to radiation therapy or chemotherapeutic alkylating agents. *Biomater. Artif. Cells Immobil. Biotechnol.* **20**, 657–660 (1992).
8. Teicher, B. A., Herman, T. S., Hopkins, R. E. & Menon, K. Effect of oxygen level on the enhancement of tumor response to radiation by perfluorochemical emulsions or a bovine hemoglobin preparation. *Int. J. Radiat. Oncol. Biol. Phys.* **21**, 969–974 (1991).
9. Teicher, B. A. *et al.* Oxygenation of the rat 9L gliosarcoma and the rat 13672 mammary carcinoma with various doses of a hemoglobin solution. *Artif. Cells Blood Substit. Immobil. Biotechnol.* **22**, 827–833 (1994).
10. Teicher, B. A. *et al.* Oxygenation of tumors by a hemoglobin solution. *J. Cancer Res. Clin. Oncol.* **120**, 85–90 (1993).
11. Teicher, B. A., Holden, S. A., Menon, K., Hopkins, R. E. & Gawryl, M. S. Effect of hemoglobin solution on the response of intracranial and subcutaneous 9L tumors to antitumor alkylating agents. *Cancer Chemother. Pharmacol.* **33**, 57–62 (1993).
12. Teicher, B. A. *et al.* Influence of an anti-angiogenic treatment on 9L gliosarcoma: oxygenation and response to cytotoxic therapy. *Int. J. Cancer* **61**, 732–737 (1995).
13. Palmer, A. F. & Intaglietta, M. Blood substitutes. *Annu. Rev. Biomed. Eng.* **16**, 77–101 (2014).
14. Kim, H. W. & Greenburg, A. G. *Hemoglobin-Based Oxygen Carriers as Red Cell Substitutes and Oxygen Therapeutics* (Springer, Berlin, 2013).
15. Baek, J. H. *et al.* Down selection of polymerized bovine hemoglobins for use as oxygen releasing therapeutics in a Guinea pig model. *Toxicol. Sci.* **127**, 567–581 (2012).
16. Belcher, D. A. *et al.* Mixtures of tense and relaxed state polymerized human hemoglobin regulate oxygen affinity and tissue construct oxygenation. *PLoS ONE* **12**, e0185988 (2017).
17. Belcher, D. A., Cuddington, C. T., Martindale, E. L., Pires, I. S. & Palmer, A. F. Controlled polymerization and ultrafiltration increase the consistency of polymerized hemoglobin for use as an oxygen carrier. *Bioconjug. Chem.* https://doi.org/10.1021/acs.bioconjchem.9b00766 (2020).
18. Cabrales, P., Zhou, Y., Harris, D. R. & Palmer, A. F. Tissue oxygenation after exchange transfusion with ultrahigh-molecular-weight tense- and relaxed-state polymerized bovine hemoglobins. *Am. J. Physiol. Heart Circ. Physiol.* **298**, H1062–H1071 (2010).
19. Meng, F. *et al.* Comprehensive biochemical and biophysical characterization of hemoglobin-based oxygen carrier therapeutics: All HBOCs are not created equally. *Bioconjug. Chem.* **29**, 1560–1575 (2018).
20. Belcher, D. A. *et al.* The quaternary state of polymerized human hemoglobin regulates oxygenation of breast cancer solid tumors: a theoretical and experimental study. *PLoS ONE* **13**, e0191275 (2018).
21. Zhang, N., Jia, Y., Chen, G., Cabrales, P. & Palmer, A. F. Biophysical properties and oxygenation potential of high-molecular-weight glutaraldehyde-polymerized human hemoglobins maintained in the tense and relaxed quaternary states. *Tissue Eng. Part A* **17**, 927–940 (2011).
22. Winslow, R. M. Targeted O2 delivery by low-p50 hemoglobin: a new basis for hemoglobin-based oxygen carriers. *Artif. Cells Blood Substit. Biotechnol.* **33**, 1–12 (2005).
23. Vandegriff, K. D. & Winslow, R. M. Hemospan: design principles for a new class of oxygen therapeutic. *Artif. Organs* **33**, 133–138 (2009).
24. Napolitano, L. M. Hemoglobin-based oxygen carriers: first, second or third generation? Human or bovine? Where are we now?. *Crit. Care Clin.* **25**, 279–301 (2009).
25. Carmichael, F. J. *et al.* A phase I study of oxidized raffinose cross-linked human hemoglobin. *Crit. Care Med.* **28**, 2283–2292 (2000).
26. Buehler, P. W. *et al.* Structural and functional characterization of glutaraldehyde-polymerized bovine hemoglobin and its isolated fractions. *Anal. Chem.* **77**, 3466–3478 (2005).
27. Gundersen, S. I. & Palmer, A. F. Hemoglobin-based oxygen carrier enhanced tumor oxygenation: a novel strategy for cancer therapy. *Biotechnol. Prog.* **24**, 1353–1364 (2008).
28. Raabe, A. *et al.* No effect of the hemoglobin solution HBOC-201 on the response of the rat R1H tumor to fractionated irradiation. *Strahlenther. Onkol.* **181**, 730–737 (2005).
29. Gottschalk, A. *et al.* Influence of the hemoglobin solution HBOC-201 on tissue oxygenation in the rat R1H-tumor. *Artif. Cells. Blood Substit. Immobil. Biotechnol.* **33**, 379–389 (2005).
30. Wu, W. *et al.* Hemoglobin-based oxygen carriers combined with anticancer drugs may enhance sensitivity of radiotherapy and chemotherapy to solid tumors. *Artif. Cells Blood Substit. Biotechnol.* **37**, 163–165 (2009).

31. Liu, X. B. *et al.* Enhancement of cisplatin-based TACE by a hemoglobin-based oxygen carrier in an orthotopic rat HCC model. *Artif. Cells Nanomed. Biotechnol.* **42**, 229–236 (2014).

32. Qi, X. *et al.* A hemoglobin-based oxygen carrier sensitized Cisplatin based chemotherapy in hepatocellular carcinoma. *Oncotarget* **8**, 85311–85325 (2017).

33. Qu, J. *et al.* Preparation of artificial red cell and its application on alleviation of tumor hypoxia. *Colloids Surf. B Biointerfaces* **160**, 446–454 (2017).

34. Tveit, K. M., Fodstad Johannessen, J. V. & Olsnes, S. A human melanoma cell line established from xenograft in athymic mice. *Br. J. Cancer* **41**, 724–733 (1980).

35. Fodstad, ØY., Aamdal, S., McMenamin, M., Nesland, J. M. & Pihl, A. A new experimental metastasis model in athymic nude mice, the human malignant melanoma lox. *Int. J. Cancer* **41**, 442–449 (1988).

36. Castro, C., Ortiz, D., Palmer, A. F. & Cabrales, P. Hemodynamics and tissue oxygenation after hemodilution with ultrahigh molecular weight polymerized albumin. *Minerva Anestesiol.* **80**, 537–546 (2014).

37. Ortiz, D., Barros, M., Yan, S. & Cabrales, P. Resuscitation from hemorrhagic shock using polymerized hemoglobin compared to blood. *Am. J. Emerg. Med.* **32**, 248–255 (2014).

38. Beaney, R. P. Positron emission tomography in the study of human tumors. *Semin. Nucl. Med.* **14**, 324–341 (1984).

39. Kallinowski, F., Schlenger, K. H., Kloes, M., Stohrer, M. & Vaupel, P. Tumor blood flow: the principal modulator of oxidative and glycolytic metabolism, and of the metabolic micromilieu of human tumor xenografts in vivo. *Int. J. Cancer* **44**, 266–272 (1989).

40. Vaupel, P., Kallinowki, F. & Okunieff, P. Blood flow, oxygen and nutrient supply, and metabolic microenvironment of human tumors: a review. *Cancer Res.* **49**, 6449–6465 (1989).

41. Yu, M. H. *et al.* Influence of PEG-conjugated hemoglobin on tumor oxygenation and response to chemotherapy. *Artif. Cells Blood Substit. Biotechnol.* **36**, 551–561 (2008).

42. Zhao, Y. *et al.* A novel nanoparticle drug delivery system based on PEGylated hemoglobin for cancer therapy. *Drug Deliv.* **26**, 717–723 (2019).

43. Murayama, C. *et al.* Liposome-encapsulated hemoglobin enhances chemotherapy to suppress metastasis in mice. *Artif. Organs* **38**, 656–661 (2014).

44. Liou, G. Y. & Storz, P. Reactive oxygen species in cancer. *Free Radic. Res.* **44**, 479–496 (2010).

45. Korde Choudhari, S., Chaudhary, M., Bagde, S., Gadbail, A. R. & Joshi, V. Nitric oxide and cancer: a review. *World J. Surg. Oncol.* **11**, 118 (2013).

46. Olson, J. S. *et al.* NO scavenging and the hypertensive effect of hemoglobin-based blood substitutes. *Free Radic. Biol. Med.* **36**, 685–697 (2004).

47. Yang, J. *et al.* Hypoxic tumor therapy by hemoglobin-mediated drug delivery and reversal of hypoxia-induced chemoresistance. *Biomaterials* **182**, 145–156 (2018).

48. Palmer, A. F., Sun, G. & Harris, D. R. Tangential flow filtration of hemoglobin. *Biotechnol. Prog.* **25**, 189–199 (2009).

49. Arifin, D. R. & Palmer, A. F. Determination of size distribution and encapsulation efficiency of liposome-encapsulated hemoglobin blood substitutes using asymmetric flow field-flow fractionation coupled with multi-angle static light scattering. *Biotechnol. Prog.* **19**, 1798–1811 (2003).

50. Hawk, P. B. *Hawk's Physiological Chemistry* 14th edn, 1090–1099 (McGraw-Hill, New York, 1965).

51. Rameez, S. & Palmer, A. F. Simple method for preparing poly(ethylene glycol)-surface-conjugated liposome-encapsulated hemoglobins: Physicochemical properties, long-term storage stability, and their reactions with O_2, CO, and NO. *Langmuir* **27**, 8829–8840 (2011).

52. Rameez, S., Banerjee, U., Fontes, J., Roth, A. & Palmer, A. F. Reactivity of polymersome encapsulated hemoglobin with physiologically important gaseous ligands: oxygen, carbon monoxide, and nitric oxide. *Macromolecules* **45**, 2385–2389 (2012).

53. Rameez, S. *et al.* Encapsulation of hemoglobin inside liposomes surface conjugated with poly(ethylene glycol) attenuates their reactions with gaseous ligands and regulates nitric oxide dependent vasodilation. *Biotechnol. Prog.* **28**, 636–645 (2012).

54. Cuddington, C., Moses, S., Belcher, D., Ramesh, N. & Palmer, A. Next-generation polymerized human hemoglobins in hepatic bioreactor simulations. *Biotechnol. Prog.* https://doi.org/10.1002/btpr.2958 (2020).

55. Cabrales, P., Tsai, A. G., Frangos, J. A. & Intaglietta, M. Role of endothelial nitric oxide in microvascular oxygen delivery and consumption. *Free Radic. Biol. Med.* **39**, 1229–1237 (2005).

56. Dufu, K. *et al.* GBT1118, a potent allosteric modifier of hemoglobin O_2 affinity, increases tolerance to severe hypoxia in mice. *Am. J. Physiol. Circ. Physiol.* **313**, H381–H391 (2017).

57. Cabrales, P., Meng, F. & Acharya, S. A. Tissue oxidative metabolism after extreme hemodilution with PEG-conjugated hemoglobin. *J. Appl. Physiol.* **109**, 1852–1859 (2010).

58. Kerger, H. *et al.* pO_2 measurements by phosphorescence quenching: characteristics and applications of an automated system. *Microvasc. Res.* **65**, 32–38 (2003).

59. Vanderkooi, J. M., Maniara, G., Green, T. J. & Wilson, D. F. An optical method for measurement of dioxygen concentration based upon quenching of phosphorescence. *J. Biol. Chem.* **262**, 5476–5482 (1987).

60. Ortiz, D., Briceño, J. C. & Cabrales, P. Microhemodynamic parameters quantification from intravital microscopy videos. *Physiol. Meas.* **35**, 351–367 (2014).

61. Wallace, M. *et al.* Enzyme promiscuity drives branched-chain fatty acid synthesis in adipose tissues. *Nat. Chem. Biol.* **14**, 1021–1031 (2018).

Acknowledgements

Author contributions

D.B. wrote the main manuscript text and prepared the figures. D.B. and A.L. performed the experiments and analyzed the data. P.C .and A.P. reviewed and revised the manuscript. All authors contributed to the design and implementation of the experiment. All authors reviewed the manuscript.

Competing interests

The authors declare no competing interests.

Additional information

Correspondence and requests for materials should be addressed to A.F.P.

Reprints and permissions information is available at www.nature.com/reprints.

Publisher's note Springer Nature remains neutral with regard to jurisdictional claims in published maps and institutional affiliations.